Capability Curve-Based Generator Protection Minimizes Generator Stress and Maintains Power System Stability

Matchyaraju Alla, Armando Guzmán, Dale Finney, and Normann Fischer
Schweitzer Engineering Laboratories, Inc.

Capability Curve-Based Generator Protection Minimizes Generator Stress and Maintains Power System Stability

Matchyaraju Alla, Armando Guzmán, Dale Finney, and Normann Fischer,
Schweitzer Engineering Laboratories, Inc.

Abstract—**Loss of field (LOF) refers to insufficient excitation for proper generator operation, causing the generator to operate outside the generator capability curve (GCC). Fast disconnection of the generator during this condition minimizes stress to the generator and maintains power system stability. This paper presents implementation details of a generator protection scheme with characteristics tailored to the machine GCC. The proposed scheme provides improved generator protection and simplifies coordination of scheme elements with the generator underexcitation limiter (UEL). The paper uses actual field events to show the performance of the proposed scheme and traditional elements under LOF conditions.**

I. INTRODUCTION

A loss of field (LOF) condition can occur because of an open or short circuit in the field circuit, an excitation failure, an operation error, or a loss of auxiliary power supply services. An LOF condition can be partial or complete. The response of the generator to LOF conditions is often impacted by generator prefault loading and by the strength of the power system. The potential to damage the generator and/or lose power system stability greatly depends on these factors. Consequently, the design and application of LOF protection are one of the more challenging aspects of generator protection.

A. Effect of an LOF on a Synchronous Generator

Reduction of the field current weakens the magnetic coupling between the stator and rotor and can lead to a loss of synchronism. If the generator loses synchronism, it will overspeed and operate asynchronously. The prefault loading is a determining factor in the final value of slip. Slip induces damaging currents into the amortisseur (damper) windings of the rotor and the body of the rotor. It can also induce high voltage into the field winding for an open field circuit, which could result in insulation damage of the field winding. The turbines that drive cylindrical-rotor generators are often very sensitive to overspeed and can be damaged quickly. While slipping poles, the generator can absorb reactive power equal to as much as twice its rated megavolt-amperes (MVA). This increase in power absorption can quickly overload the stator.

Fig. 1 shows a cut-away view of a cylindrical-rotor generator. When the field current decreases, the rotor retaining rings that hold the field winding transition from a saturated state to an unsaturated state. As a result, the reluctances of the paths between the core ends and the rotor decrease. This decrease results in increased fringe, axial flux flowing between the stator-end-core regions and the rotor retaining rings [1].
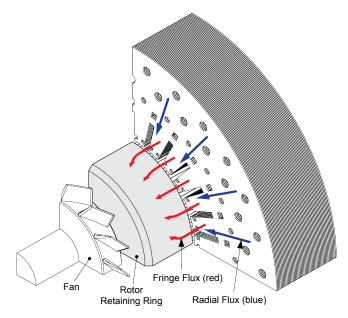

Fig. 1.   The fringe flux (shown in red) between the stator-end-core region and the retaining ring increases when the rotor retaining ring comes out of saturation.

The fringe flux linking the stator core rotates at the generator synchronous speed, but it is stationary with respect to the rotor. Therefore, the fringe flux causes circulation of eddy currents and losses in the stator-end-core laminations; there is neither circulation of eddy currents nor losses in the rotor retaining rings. The generator stator core is designed to carry radial flux parallel to the stator-core laminations. To reduce eddy currents in the stator core, the stator core is composed of thinly laminated sheets of cold-rolled, grain-orientated silicon steel. However, when the rotor retaining rings come out of saturation, the flow of fringe flux between the stator-end-core regions and the rotor retaining rings increases. This fringe flux at the stator-end-core regions flows perpendicularly (axially) to the stator lamination. The area of the lamination perpendicular to the fringe flux is now large, so eddy current losses will be far greater than those produced by the radial flux that flows parallel to the stator laminations, as shown in Fig. 2.
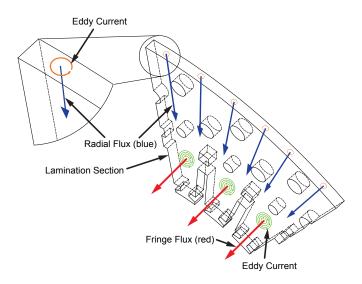
Fig. 2.   Eddy currents caused by the fringe flux circulate at the stator-end-core regions.

The heat generated by the fringe flux is high enough to melt the stator-core lamination within minutes. The amount of reactive power that a cylindrical-rotor synchronous generator can absorb is determined by the heat that the stator-end-core region can dissipate before being damaged. Hence, the reactive power lower limit of the generator capability curve (GCC) for cylindrical-rotor synchronous generators is determined by the stator end-core heating limit (SECHL) and not by the stator current heating limit. It is important to note that the end-core heating phenomenon described previously does not occur in salient-pole generators.

B.   Effect of LOF on the Power System

As mentioned previously, the generator draws a significant amount of reactive power to maintain the magnetic field during an LOF event. This reactive power consumption can jeopardize the stability of the power system.

A loss of synchronism can cause large pulsations in voltage and current that can further jeopardize the power system and negatively impact stability.

II.   GENERATOR CAPABILITY CURVE

The GCC defines the generator operating limits in the P-Q plane, as shown in Fig. 3. The following factors determine the GCC:

1.   The current rating (thermal limit) of the field winding imposes the limit on the generator reactive power export capability (GCC overexcited region, Segment 1 in Fig. 3).
2.   The current rating (thermal limit) of the stator winding imposes the limit on the generator active power output at near unity power factor (Segment 2 in Fig. 3).

3.   The generator type determines the GCC underexcited region limit (Segment 3 in Fig. 3):
   a)   SECHL limits the reactive power import of most cylindrical-rotor generators.
   b)   The current rating (thermal limit) of the stator winding limits the underexcited region of salient-pole generators. Salient-pole generators with direct-axis synchronous reactance, X_d, less than 1.0 pu only have two limits (Segments 1 and 2 shown in Fig. 3). However, the steady-state stability limit (SSSL) is generally more restrictive than the stator winding thermal limit of the generator and therefore typically defines the generator underexcitation limit.
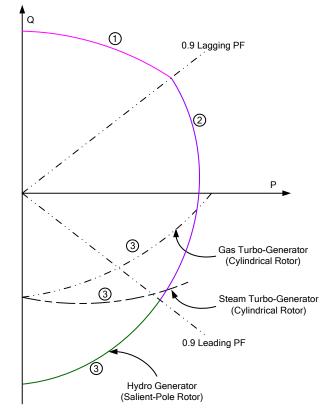

Fig. 3.   GCCs for cylindrical-rotor and salient-pole-rotor generators.

A.   Effect of Coolant Pressure and Terminal Voltage on the Dynamic Capability Curve

1)   Effect of Coolant Pressure on GCC

Synchronous generators can have multiple ratings depending on their cooling, such as coolant temperature (e.g., ambient air) or coolant pressure (e.g., hydrogen). Generator manufacturers specify the GCC based on coolant temperature or pressure typically above and below the generator-rated temperature or pressure, as shown in Fig. 4. The higher the coolant pressure, the greater the operating range of the generator and vice versa.
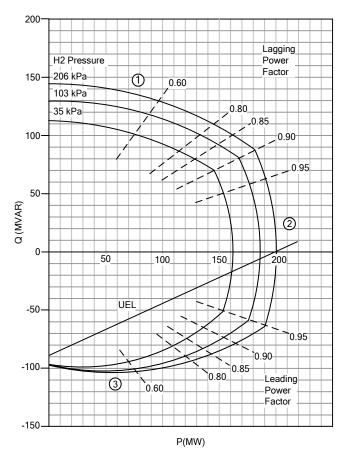
Fig. 4. GCC at nominal voltage of a 202 MVA, 15 kV, 0.9 pf, 3600 rpm, 60 Hz, hydrogen-cooled steam-turbine generator for various hydrogen pressures.

2) Effect of Terminal Voltage on the Generator Underexcited Region

Utility generators in North America are typically designed in accordance with [2] and [3] to operate at voltages between 95 percent and 105 percent of the nameplate (nominal) voltage. This requirement is subject to the confines of the reactive power capability and the allowable temperature rise of the generator [4]. To illustrate the effect of the terminal voltage (V_T) on the generator underexcited region, we use the simplified steady-state equivalent circuit of a synchronous generator connected to a power system shown in Fig. 5.
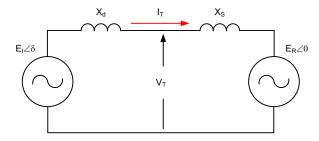

Fig. 5. Simplified equivalent circuit of a synchronous generator connected to a power system.

The internal voltage (E_I) is the sum of V_T and the voltage drop across X_d. E_I is directly proportional to the field current (I_{FD}). Lower I_{FD} translates to increased end-core heating.

Manufacturers provide GCCs at $V_T = 1$ pu; we use these curves, along with the relationship stated in the previous paragraph, to estimate the GCC at other V_T magnitudes. Fig. 6 shows an example that uses the GCC from Fig. 4 and $X_d = 1.54$ pu to illustrate the relationship between V_T and I_{FD}. When this generator is loaded in excess of 0.4 pu of its rating, I_{FD} at $V_T = 1.05$ pu is slightly lower than when it operates at $V_T = 1.0$ pu.
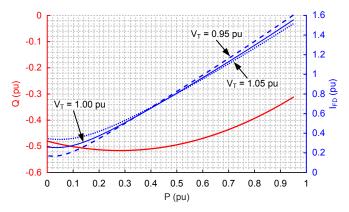

Fig. 6. Field currents at off nominal voltage can be lower than currents at $V_T = 1.00$ pu for certain loading conditions.

For cylindrical-rotor generators, the reactive power absorption capability of the generator generally decreases with an increase in V_T. Equations (1) and (2) are an approximation of this phenomenon [5], which is illustrated in Fig. 7 [6].

$$\text{Center}(P,Q) = \left(0, \frac{k_1 \cdot V_T^2}{X_d} \right) \qquad (1)$$

$$\text{Radius} = \frac{k_2 \cdot V_T}{X_d} \qquad (2)$$

where:
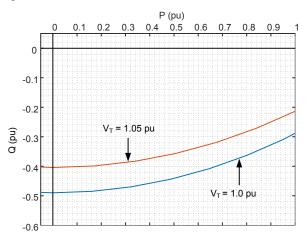 k_1 and k_2 are thermal constants, which vary among generators.

Fig. 7. Variation of reactive power absorption capability with terminal voltage, V_T.

III. Stability Limits and UEL

Stability limits are important because an LOF will often result in a loss of stability. This section discusses why it is necessary to coordinate the UEL and SSSL characteristics with the LOF protection elements of the generator.

A. Stability Limits

Synchronous generators have two different generator stability limits that depend on the automatic voltage regulator (AVR) operating mode (manual or automatic). The SSSL is the limit when the AVR operates in manual mode. The dynamic stability is the limit when the AVR operates in automatic mode.

1) Steady-State Stability Limit

The SSSL can best be understood by using the simplified power-angle equation as applied to a generator. Referring to Fig. 5 and ignoring rotor saliency, we can write the power-angle equation as (3).

$$P = \frac{|E_I| \bullet |E_R| \sin \delta}{X_d + X_S} \tag{3}$$

where:

E_R is the remote source voltage.

δ is the load angle.

X_S is the power system impedance.

When the AVR is in manual mode, E_I is fixed. For a constant E_I, if P is increased, then δ must increase to balance (3), assuming that E_R is constant. At $\delta = 90°$, the right side of (3) is at maximum. A further power increase results in a loss of steady-state stability. Note that the SSSL depends mainly on X_d and X_S.

The equations for the SSSL are defined in the P-Q plane, as shown in Fig. 8 [6]. The SSSL characteristic in the P-Q plane varies with the square of V_T. The generator is connected to a power system, in which X_S changes. Therefore, as shown in Fig. 8, the SSSL characteristic changes with the system strength. Note also that SSSL can be considered a worst-case scenario because it only applies if the AVR is in manual mode [7]. However, an AVR with a power system stabilizer (PSS) improves the stability limits substantially, as the next subsection describes.

2) Dynamic Stability Limit

In the previous subsection, the generator E_I was fixed because the AVR was in manual mode. DeMello et al. [8] developed a linearized generator model to account for the variations in E_I that occur when the AVR is in automatic mode. According to this development, the electrical torque is resolved into two components: a synchronizing component that is proportional to a deviation in δ and a damping component that is proportional to a deviation in speed.

With a constant E_I, there is no damping torque limit; the synchronizing torque is the only limit.

Insufficient synchronizing torque results in a loss of steady-state stability as described in the previous subsection.

Insufficient damping torque results in dynamic instability. This instability can be characterized as a growing (undamped) oscillation over time.
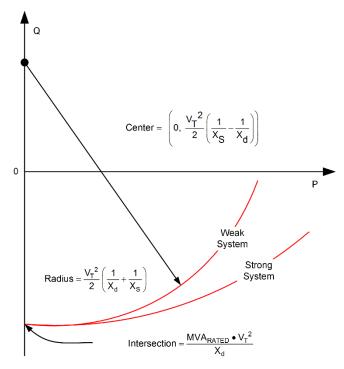

Fig. 8. Variation of the SSSL characteristic with power system strength.

Benmouyal [7] describes a method that uses eigenvalues for characterization of dynamic stability. Using this method, one can plot dynamic stability limits in the P-Q plane for various values of AVR gain (Ke), as shown in Fig. 9. Following an external fault clearance, it is necessary to have the highest excitation voltage possible in the shortest possible time for the generator field to contribute positively to the generator transient stability. Such a contribution is feasible with high-speed exciters. This condition implies that Ke should be as high as possible. However, high Ke decreases the damping torque, causing the generator to experience oscillations. Note that the dynamic limit with high Ke can be more restrictive than the SSSL, as Fig. 9 illustrates.

a) Impact of AVR and PSS on System Stability

To address the reduction in damping torque, high-speed exciters are equipped with PSSs. The effect of a PSS is to increase the damping torque artificially to improve the dynamic stability limit. Fig. 9 shows the improvement. When Ke = 50 (without PSS), the dynamic stability limit is within the generator theoretical maximum capability curve (GTMC), which is a stator current, 1 pu radius circle. With the addition of the PSS, the generator can be operated at its full capacity. For this example, Ke could be set to 200 or higher without compromising the normal operation of the generator. The characteristics shown in Fig. 9 provide a useful visualization of the control system behavior in the P-Q plane, but they do not replace the need for dynamic simulations to coordinate protection and control system response [9].
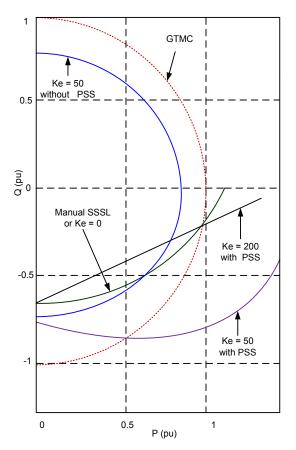
Fig. 9.   Impact of PSS on generator stability limit.

B.   Underexcitation Limiter

UELs were introduced in the late 1940s when power system stability became a major concern. UELs were intended to prevent generator operation beyond the SSSL or SECHL. Therefore, the UEL characteristic should be set according to the SSSL or SECHL, whichever is more restrictive [10]. The impact of V_T on the UEL setting depends on the AVR manufacturer. Some UEL characteristics are not affected by changes in V_T, while others are a function of V_T.

If SECHL is the most restrictive curve, the UEL characteristic may be set to follow this characteristic with minimal margin (e.g., 5 percent to 10 percent of rated MVA). A brief excursion beyond the limit may be allowable. In the unlikely event that the calculated SSSL is used as the basis for

the UEL setting, margin may not be necessary because of the conservative method used for calculating this limit [4]. The LOF protection element and UEL characteristics should be coordinated so that the LOF element allows the UEL sufficient time to respond to an underexcited condition.

C.   AVR Redundancy

As discussed previously, the excitation system typically has two operating modes: automatic and manual. A failure of the AVR or one of its inputs (a VT fuse failure, for example) usually causes the excitation system to failover from automatic to manual mode. Under automatic operation, the SSSL does not apply but, because of the possibility of failover, it has been typical to coordinate the UEL characteristic with the SSSL characteristic. This coordination restricts generator underexcited operation even in automatic mode. Redundant AVRs have been implemented recently on some generators [6]. Because of the low probability of both AVRs failing, the SSSL may rarely be the operative limit.

IV.   GCC, UEL, AND SSSL CHARACTERISTICS IN THE P-Q, ADMITTANCE, AND IMPEDANCE PLANES

Generator and AVR data typically include GCC and UEL characteristics in the P-Q plane, and the SSSL characteristic is represented in the impedance plane because it depends on generator and power system impedances and is voltage invariant. These characteristics must be presented in a common plane when setting and analyzing the performance of LOF elements. Through use of proper transformations between planes, we can represent the GCC, UEL, and SSSL characteristics simultaneously in the P-Q, admittance, or impedance planes.

A.   P-Q Plane

To obtain the GCC and UEL characteristics in the pu P-Q plane, we divide the values that define these characteristics by the generator-rated MVA.

Fig. 10 (a) shows the GCC and UEL characteristics in the pu P-Q plane. They correspond to the characteristics depicted in Fig. 4. Fig. 10 (a) also shows the SSSL characteristic that corresponds to the same generator that has $X_d = 1.54$ pu and a power system with $X_S = 0.298$ pu. Notice that the underexcited region is on the left-hand side of Fig. 10 (a).
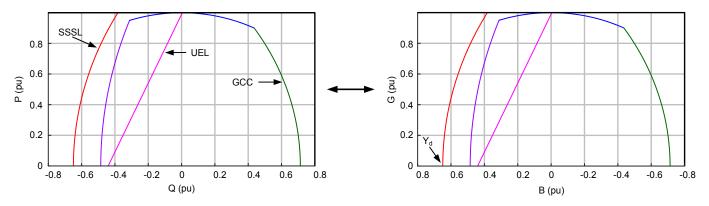

Fig. 10.   GCC, UEL, and SSSL characteristics in the pu P-Q plane (a) and admittance plane (b).

B. Admittance Plane

We use the P-Q plane characteristics and (4) to obtain the corresponding characteristics in the pu admittance plane (Y).

$$Y = \frac{S*}{V_T^2} \bullet Z_{BASE} = G + jB \qquad (4)$$

where:

V_T is the terminal voltage in kV.

S is the complex power in MVA.

* indicates complex conjugate.

Z_{BASE} is the generator base impedance in ohms.

G is conductance in pu.

B is susceptance in pu.

Fig. 10 (b) shows the admittance plane representation of the characteristics depicted in Fig. 10 (a). Note that the characteristics represented in the pu P-Q plane have the same shape and form as the characteristics represented in the pu admittance plane. In Fig. 10 (b), the values of B increase toward the left of the horizontal axis. The pu value of the direct-axis synchronous admittance $Y_d = 1/X_d = 0.65$ pu, as Fig. 10 (b) illustrates.

C. Impedance Plane

We use the P-Q plane characteristics in MVAs and (5) to obtain the corresponding characteristics in the pu impedance plane.

$$Z = \frac{V_T^2}{S* \bullet Z_{BASE}} = R + jX \qquad (5)$$

where:

R is resistance in pu.

X is reactance in pu.

The SSSL characteristic in the impedance plane for an ideal lossless system with a generator connected to a power system is a circle described by (6).

$$Z_{SSSL}(\alpha) = \left(\frac{1}{X_d} + \frac{1}{X_S}\right) \bullet e^{j\alpha} + j\left(\frac{1}{X_d} - \frac{1}{X_S}\right) \qquad (6)$$

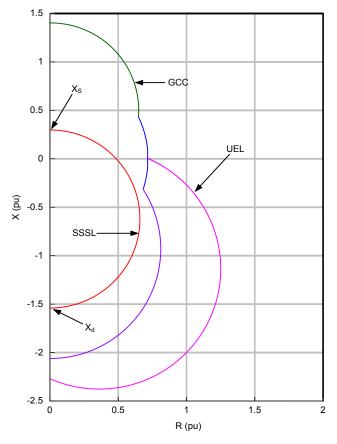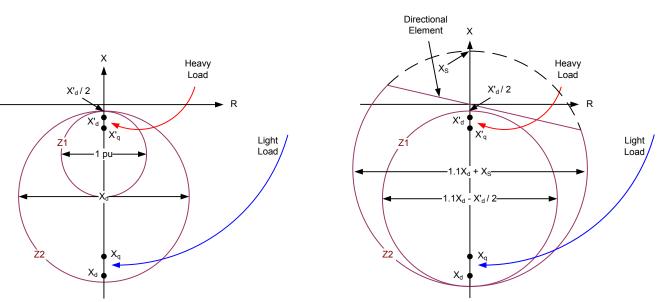Fig. 11 shows the impedance plane representation of the characteristics depicted in Fig. 10 (a) and Fig. 10 (b).

Fig. 11. GCC, UEL, and SSSL characteristics in the pu impedance plane that correspond to the characteristic shown in Fig. 10 (a) and Fig. 10 (b).

V. CURRENT PRACTICE OF LOF PROTECTION

A. Impedance-Based Loss-of-Field Protection

Impedance-based protection is one of the earliest applied methods for detection of LOF events [11]. Impedance-based LOF elements respond to the apparent impedance, Z_{APP}. Prior to an LOF condition, the Z_{APP} looking toward the generator is defined by the generator loading. From Fig. 5, it is evident that Z_{APP} is approximately equal to X_d for a complete LOF ($E_I = 0$). If the generator loses synchronism during an LOF event, the generator rotor speed increases and the Z_{APP} approaches the direct-axis transient reactance, X'_d. For salient-pole generators, as the machine slips poles, the Z_{APP} of the machine varies between X_d and the quadrature axis synchronous reactance, X_q, if the slip is low, and between X'_d and the quadrature axis transient reactance X'_q if the slip is high.

Fig. 12.   Impedance-based LOF protection characteristics, Scheme 1 (a) and Scheme 2 (b).

The correlation between Z_{APP} and the generator impedance for an LOF event motivated the design of early LOF schemes that used a single relay with an offset-mho characteristic set to encircle both X_d and X'_d. Over time, as generator designs improved, the X_d values increased to 1.5–2.2 pu. The resulting increase in the required diameter of the mho characteristic created the concern that it could encroach into the GCC underexcited region. This led to the development of the dual-zone impedance schemes [12].

Fig. 12 presents the two schemes included in [13]. For each method, Fig. 12 shows the basic guidelines for setting the impedance offsets and diameters. Note that these guidelines meet the criteria of encircling X_d and X'_d. IEEE Standard C37.102 [13] provides the following setting guidelines.

1) Scheme 1

The Zone 1 (Z1) element is intended to provide fast clearing for an LOF at heavy load. The Zone 1 delay is set at several cycles (e.g., six cycles [14]). The reduced coverage of this zone provides security for stable power swings. Zone 2 (Z2) is intended to detect an LOF at light load. The greater coverage for this zone makes it more susceptible to power swings, so the delay is typically set at 30 to 45 cycles.

2) Scheme 2

The Zone 1 element is also intended to provide fast clearing for an LOF at heavy load. The Zone 1 delay is typically set at 15 cycles. Zone 2 includes an impedance element, a directional element, and an undervoltage element [15]. X_S is defined as the impedance of the generator step-up transformer (GSU) plus the equivalent impedance of the power system with the strongest source out of service, and it determines the forward reach. The Zone 2 element has a delay in the range of 10–60 s. Tripping of Zone 2 is accelerated 12 to 18 cycles if the undervoltage element picks up. The undervoltage element pickup is typically set at 0.8 to 0.87 pu.

B. Admittance-Based Loss-of-Field Protection

As is the case of impedance-based LOF protection, admittance-based protection has been applied for decades. The operating signals of the two methods are closely related; admittance is the multiplicative inverse of impedance.

As we discussed in Section IV, representation of the GCC in the admittance plane preserves the GCC shape during mapping of the GCC from the P-Q plane to the admittance plane. Fig. 10 illustrates this relationship.

Traditionally, the operating characteristics of LOF admittance elements are composed by straight lines in the admittance plane. Each characteristic can be defined by a susceptance value and a slope. The admittance scheme has two zones. Zone 1 is intended to coordinate with the theoretical dynamic stability limit (TDSL). This limit is derived from a solution of the two-axis, synchronous generator model in the transient state [16]. TDSL is related to the concept of dynamic stability that Section III describes, but TDSL does not consider the behavior of the generator controls. As shown in Fig. 13, the TDSL originates on the B axis at $1/X_q$ and is asymptotic to $1/X'_d$. The basic setting guidelines call for a B setting of $2/X_d$ and a slope of 110° with a recommended delay of less than 0.3 s.

Zone 2 is intended to coordinate with the theoretical steady-state stability limit (TSSL), TSSL = SSSL when $X_S = 0$. For cylindrical-rotor generators, this limit is a vertical line at $1/X_d$. For salient-pole generators, this limit originates on the B axis at $1/X_q$ and is asymptotic to $1/X_d$ [17]. Zone 2 is composed of two characteristics. For cylindrical-rotor generators, the basic setting guidelines call for the first characteristic to have a B setting of $1/X_d$ and a slope of 80° and the second characteristic to have a B setting of $0.9/X_d$ and a slope of 90°. For salient-pole generators, the basic setting guidelines call for the first characteristic to have a B setting of $1/X_d$ and a slope of 100° and the second characteristic to have a B setting of

$1/X_d + (1/X_q - 1/X_d)/2$ and a slope of 90°. The delay is set to approximately 10 s, but tripping is accelerated to 0.5–1.5 s for any detection of low field voltage [16].

In Fig. 13, Z1 and Z2 are plotted for $X_d = 1.1$, $X_q = 0.7$, and $X'_d = 0.2$. The dashed lines are solutions to the general synchronous generator equations in the synchronous state for constant I_{FD} [17]. The TSSL connects the maxima of these lines. The dot-dashed lines are solutions to the general synchronous generator equations in the transient state (X_d is replaced with X'_d) for constant I_{FD}. The TDSL connects the maxima of these lines.
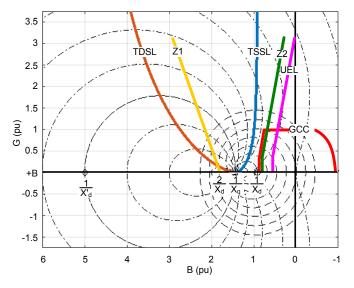

Fig. 13. Coordination of the admittance protection scheme with TSSL for a salient-pole generator.

In Fig. 14, we compare the coverage of the impedance and admittance schemes for a cylindrical-rotor generator with $X'_d = 0.25$ pu, $X_d = 1.8$ pu, and $X_S = 0.15$ pu. For a complete LOF condition, the Z_{APP} ends up between X_d and X'_d and all LOF schemes operate.
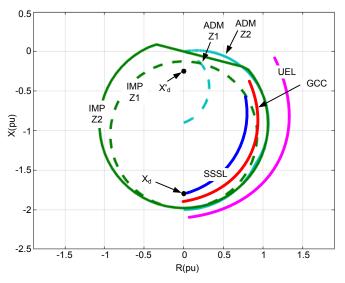

Fig. 14. Comparison of coverage for admittance and impedance protection schemes with basic setting guidelines.

The coverage of each scheme differs in some way from the coverage the other schemes provide. For example, impedance Scheme 2 Zone 1 (IMP Z1) in Fig. 14 provides more coverage than admittance Zone 1 (ADM Z1) but could be more susceptible to misoperation during stable power swings. It is important to remember that the dynamic behavior of each element is also a function of the supervising elements and time delays.

The plots shown in Fig. 14 consider only basic setting guidelines. Detailed settings go beyond the criterion of encircling X_d and X'_d. IEEE Standard C37.102 [13] requires coordination between the LOF scheme and the SSSL, GCC, and UEL characteristics. For the impedance schemes, coordination entails mapping of these curves from the P-Q plane to the impedance plane. Note that for Scheme 2, the basic Zone 2 forward and reverse reach settings ensure that this element coordinates with the SSSL characteristic, which is also a function of X_d and X_S. Similarly, the basic setting guidelines for the admittance scheme ensure coordination with the theoretical stability limits.

VI. P-Q PLANE BASED LOF ELEMENT

In this section, we describe a new LOF protection scheme based on the GCC defined in the P-Q plane. The scheme comprises three LOF protection zones and a GCC alarm zone as shown in Fig. 15.
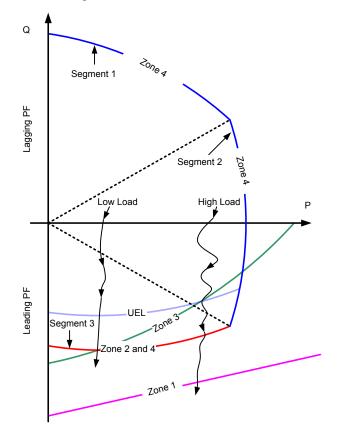

Fig. 15. P-Q based LOF protection scheme with four zones.

A. *Zone 1 Trip Element*

When an LOF condition occurs on a strong power system, the system supplies the generator with reactive power. If the generator is heavily loaded prior to the LOF condition, the generator draws a large amount of reactive power from the system. This condition could impact the generator stability as the generator transitions from synchronous to asynchronous operation. Zone 1 is defined in the P-Q plane as a straight line, but it operates in the admittance plane. As shown in Fig. 15, the operating point moves quickly into Zone 1 for these loading conditions. Zone 1 is intended to operate quickly for severe LOF events (e.g., open circuit in the field winding).

The Zone 1 characteristic and delay can be set following the traditional LOF element practice. The delay for Zone 1 is typically set short enough to prevent damage for an LOF at full load, but long enough to avoid a trip for stable power swings.

B. *Zone 2 Trip Element*

The Zone 2 element operates for LOF events at low loads. It also provides thermal protection during underexcited operation. The generator underexcited operation is governed by the UEL. There are a variety of UEL characteristics that have been modeled in [18]. In the P-Q plane, the UEL characteristic shifts proportionally to V_T^k, where k can have a value of either 0, 1, or 2.

For instance, the IEEE UEL1 characteristic is a circle that changes according to V_T^2 (k = 2). The IEEE UEL2C characteristic is either a single straight line or a multi-segmented characteristic; it can be configured to be either independent of V_T (k = 0) or dependent on V_T (k = 1) or dependent on V_T^2 (k = 2).

The Zone 2 element can be tailored according to the UEL characteristic and includes a margin and a k setting to coordinate with the UEL characteristic. Furthermore, the Zone 2 element can adapt to changes in the generator cooling capability if this adaptability is supported by the UEL.

Zone 2 delay is set short enough to prevent damage for an LOF condition at low loads but long enough to avoid tripping for stable power swings. A delay setting in the range of 1 to 60 s is recommended. As with the impedance schemes, the Zone 2 element can be set to have an accelerated trip during field or terminal undervoltage conditions. A delay in the range of 0.25 to 0.5 s may be used during undervoltage conditions (V_T < 0.8 pu as per [19]). Stable power swings or UEL dynamic response can cause Zone 2 operation during these conditions, so detailed power system studies must be performed to determine optimal delay setting.

C. *Zone 3 SSSL Alarm and Trip Element*

In weak power systems, the SSSL characteristic could encroach into the GCC. For proper coordination, the Zone 3 element is based on the replica of the SSSL characteristic and is set according to (7), where X_d and X_S are settings. The Zone 3 characteristic is defined as a circular segment in the P-Q plane

bounded within the 3rd and 4th quadrants. The characteristic is implemented in this plane but operates in the admittance plane. It is notable that some AVRs use (7) to implement the UEL characteristic.

$$Z3_{pu} = Re\left(\left(\left(P + jQ\right) - \frac{j3 \cdot V_T^2}{X_S}\right) \cdot \left(\frac{-j3 \cdot V_T^2}{X_d} - \left(P + jQ\right)\right)^*\right) \quad (7)$$

The Zone 3 characteristic will always move in synchronism with the SSSL characteristic. It therefore does not lose coordination when V_T changes.

Zone 3 picks up and instantaneously alarms when the operating point approaches or crosses the SSSL characteristic. Because loss of steady-state stability may not occur when the AVR and PSS are in service, this alarm condition can be corrected by the operator. Additionally, when Zone 3 picks up, it issues a trip command after a short delay if the AVR operates in manual mode or V_T < 0.8 pu.

It is important to note that SSSL is meaningful when the AVR operates in manual mode. If the AVR provides an indication that it is in manual mode, this indication can be routed to the Zone 3 element to supervise tripping. Alternatively, an actual loss of steady-state stability should be accompanied by a significant undervoltage condition (V_T < 0.8 pu) [19]. Therefore, Zone 3 includes a dedicated undervoltage supervision element to accelerate tripping regardless of the AVR operating mode. A pole slip can occur quickly, so the delay should be set on the order of 0.25 s.

The traditional Zone 2 element of impedance Scheme 2 is often set to coordinate with the SSSL characteristic. In the proposed scheme, Zone 3 is dedicated to coordinate with the SSSL characteristic and Zone 2 is dedicated to coordinate with the UEL characteristic. Therefore, no compromise is required when setting Zone 2.

D. *Zone 4 GCC Alarm Element*

The GCC alarm function uses the three segments identified as 1, 2, and 3 in Fig. 15 to implement a digital replica of the GCC. One of the algorithms in the scheme fits one curve for each segment of the GCC. Furthermore, the algorithm can model Segment 3 by using either piece-wise-linear or quadratic curve fitting to accommodate various GCCs with either straight-line or circular characteristics.

P and Q coordinates are used to define each segment. As Section II describes, many generators, such as that in Fig. 4, have a GCC that expands and contracts according to the generator cooling level. The algorithm is designed to shrink and expand the GCC replica based on an analog measurement of the cooling capability or a binary input (if available), as shown in Fig. 16.

In this case, the coordinates of the minimum GCC (identified with circular dots in Fig. 16) are also entered along with the coordinates of the maximum GCC (identified with diamonds in Fig. 16).
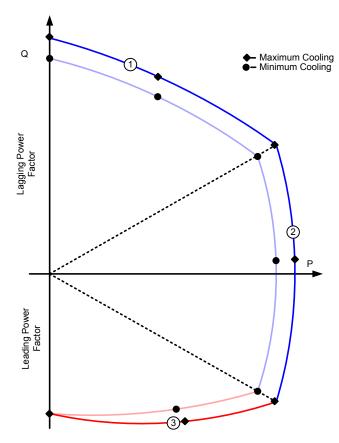
Fig. 16.   Adaptive GCC replica based on the generator cooling capability.

The Zone 4 element is intended to provide an alarm whenever the generator operates close to the GCC limits. This element does not trip the generator, so its delay can be set in the range of 1–10 s to minimize the occurrence of spurious assertions.

Segment 3 of Zone 4 can be set between the UEL and Zone 2 characteristics to issue an alarm before the operating point reaches Zone 2. Segment 3 dynamically coordinates with the UEL and Zone 2 characteristics based on the k setting. A properly configured Zone 4 characteristic can also vary with the generator cooling capability.

E. Coordination of LOF Elements With the UEL Characteristic During Terminal Voltage Variations

Fig. 17 shows one approach for coordination of Zone 2, Zone 4, and UEL characteristics with k = 0. In this approach, let us consider a voltage-independent UEL (k = 0) with a two-straight-line characteristic set with a 10 percent margin with respect to Segment 3 of the GCC as described in Table II of the Appendix. According to the proposed scheme, Zone 2 follows the UEL settings but, because it has a margin setting of 10 percent, it is situated at Segment 3 of the GCC. Optionally, for alarming, Segment 3 of Zone 4 can be set with 5 percent margin with respect to the GCC. For k = 0, the UEL, Zone 2, and Zone 4 characteristics are static in the P-Q plane, and the Zone 3 characteristic varies in proportion to V_T^2.
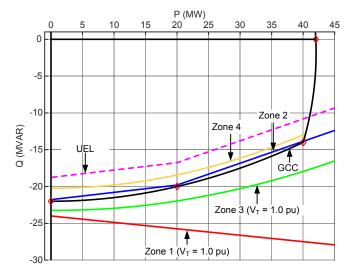

Fig. 17.   UEL and LOF characteristics for k = 0.

Fig. 18 shows the coordination of Zone 2 and UEL characteristics for the k = 1 setting as described in Table III of the Appendix. The figure also shows the UEL and Zone 2 characteristics for $V_T = 1$ and 0.85 pu, and the Zone 3 characteristic for $V_T = 0.85$ pu. Note that the Zone 2 characteristic moves the same way as the UEL characteristic.
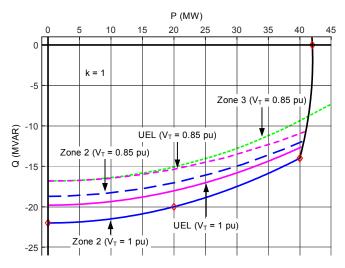

Fig. 18.   UEL and LOF characteristics for k = 1.

When $V_T < 0.8$ pu and the operating point is inside the Zone 3 characteristic, if the AVR fails to correct the low voltage condition, Zone 3 times out and issues a trip command to prevent the generator from slipping poles. With this approach, schemes with k = 0 or k = 1 accelerate tripping during severe undervoltage conditions (e.g., $V_T < 0.8$ pu) via Zone 3.

SECHL changes according to (1) and (2), so the UEL characteristic should be set above the SECHL at $V_T = 1.05$ pu for proper coordination when k = 2, as shown in Fig. 19. Therefore, the margin between the UEL characteristic and the GCC should be no less than 15 to 20 percent at $V_T = 1.0$ pu.

Zone 2 should be set with respect to UEL with a margin of 5 to 10 percent to protect the generator when 1.0 pu $< V_T \leq$ 1.05 pu. With this margin, Zone 2 provides protection for end-core heating during overvoltage conditions, but it decreases the generator operating capability at rated voltage. This problem is typically more pronounced in combustion gas turbines where the SECHL is extremely restrictive, as shown in Fig. 3. If, however, Zone 2 is set to match the GCC, it will not provide protection for the generator when 1.0 pu $< V_T \leq$ 1.05 pu (see the highlighted portion in Fig. 19).
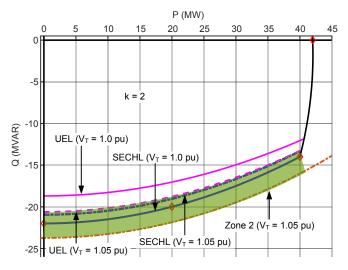

Fig. 19.   UEL characteristic for k = 2 and SECHL.

In summary, the key features of the proposed LOF protection and monitoring scheme are as follows:

- All the zones are set in the P-Q plane, using the generator GCC and data sheet.
- Zone 1 and Zone 3 operate in the admittance plane and account for changes in V_T.
- Zone 2 and Segment 3 of the Zone 4 characteristic coordinate with the UEL characteristic by means of their k corresponding settings.
- Zone 2 trip can be accelerated during severe LOF conditions accompanied by undervoltage ($V_T < 0.8$ pu).
- Zone 3 issues an alarm when the operating point approaches or crosses the SSSL characteristic and issues a trip during undervoltage conditions ($V_T < 0.8$ pu).
- Zone 3 can also trip with a short delay when the AVR operates in manual mode.
- Studies for determining proper delay settings of Zone 1 and accelerated Zone 2 (when k = 2) and Zone 3 should be performed in the admittance plane.

VII.   PERFORMANCE ANALYSIS USING FIELD EVENTS

A.   Case Study 1: SSSL Violation During Black Start Testing

Sosa et al. [14] analyzed an LOF operation during a black start test. The operation occurred while the operator was increasing the generator power output and the AVR was inadvertently operating in manual mode. Their analysis was based on the generator voltage, V_T, and current, I_T, waveforms captured during this event, which are shown in Fig. 20. The gaps between the traces are related to the periods where the relay did not capture event data. From these signals, we can infer that the oscillations caused significant stress on the generator shaft. The active and reactive power oscillations can also be seen in Fig. 20. Next, we use the impedance and P-Q planes to analyze this event in detail.
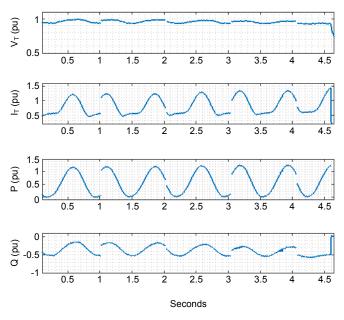

Fig. 20.   Generator oscillations while the AVR was in manual mode: V_T, I_T, P, and Q.

Fig. 21 shows the trajectory of the operating point in the impedance plane during this event. At the beginning of the event, the operating point moved into Zone 2 and Zone 1, but it did not remain in either zone longer than the corresponding zone delay setting. Later, when the operating point stayed inside Zone 2 long enough for the timer to expire, the relay issued a trip command to the generator breaker.
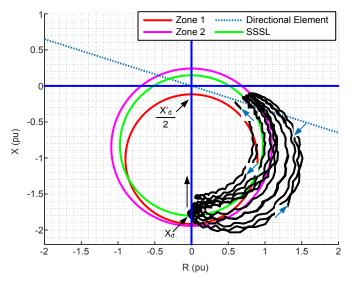

Fig. 21.   Impedance trajectory during an LOF event while the AVR was in manual mode.

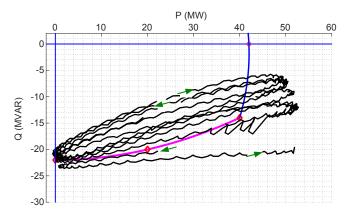Fig. 22 shows the complex power in the P-Q plane for the same event.

Fig. 22. Complex power trajectory during an LOF event while the AVR was in manual mode.

The active and reactive power output of the generator under quasi-steady-state conditions (negligible slip) can be calculated using (8) and (9), respectively.

$$P = \frac{E_I E_R}{X_d + X_S} \sin\delta + E_R^2 \frac{X_d - X_q}{2(X_d + X_S) \cdot (X_q + X_S)} \sin 2\delta \qquad (8)$$

$$Q = \frac{E_I E_R}{X_d + X_S} \cos\delta - E_R^2 \left(\frac{\cos^2\delta}{X_d + X_S} + \frac{\sin^2\delta}{X_q + X_S} \right) \qquad (9)$$

The active power output of any generator is governed by (8). During transient conditions, the generator power capability (the curve labeled E'_I in Fig. 23) is higher than during steady-state conditions due to the decrease in X_d.
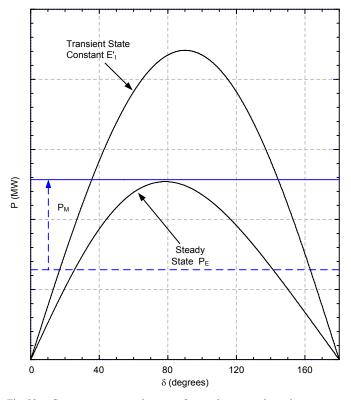

Fig. 23. Generator power-angle curves for steady-state and transient state conditions.

With the AVR inadvertently left in manual mode, the mechanical power, P_M, input to the generator was increased (as shown by the blue lines in Fig. 23). In manual mode, I_{FD} is held constant. This results in a constant E_I of the machine, so the power-angle curve cannot change dynamically. For the electrical output power, P_E, to match P_M, δ must increase.

When there is a power mismatch between P_E and P_M, the generator starts to slip. This slip causes additional induced voltage in the rotor circuit, which tends to maintain the direct-axis field in the machine. The reactive power absorption increases until $\delta = 90°$, for which it reaches approximately V_T^2 / X_d.

Because of the additional induced electromotive force (EMF) in the rotor field circuit and damper bars, the reactive power the generator absorbs for δ greater than 90° continues to increase. Therefore, the generator absorbs the maximum reactive power when $160 < \delta < 180°$. If the induced rotor EMF increases, the generator opposes any increase in the rotor angle resulting from the damping torque. Just before δ reaches 180°, the stator pole (N_{STATOR}) pushes the rotor pole (N_{ROTOR}) away, as shown in Fig. 24 (b). Pushing the rotor back toward the stator no-load position (S_{STATOR}), as shown in Fig. 24 (a), maintains the generator synchronism. The stator pole pushing the rotor pole away occurs only if the field excitation is small but non-zero. With the rotor approaching the no-load position ($\delta \approx 0°$), the generator active power export decreases, the rotor begins to accelerate, δ increases, and the generator increases its active power output.
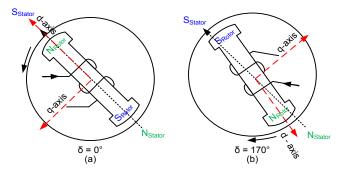

Fig. 24. Relative position of the stator and rotor fields for $\delta = 0°$ (a) and $\delta = 170°$ (b).

These slip changes cause Z_{APP} to deviate from X_d. Denoting the instantaneous direct-axis reactance as $X_d(t)$, we can state that $X'_d < X_d(t) < X_d$. With $X_d(t)$ changing (as shown in Fig. 21), the power-angle curve also changes. The generator is therefore capable of transiently delivering active power in excess of its nameplate rating, as shown in Fig. 20 and Fig. 22. This oscillation of δ continues until either the magnetic field between the stator and rotor is increased or the generator begins slipping poles.

For a black start test condition, X_S may be large (weak system). The SSSL characteristic can therefore be well within the GCC. Setting Zone 2 to address this condition restricts the generator operation capacity. As shown in Fig. 17, Zone 3 is designed to deal with conditions when the AVR is inadvertently switched to manual mode or is set in manual mode. Zone 3 is intended to alarm the operator that the generator is approaching

the SSSL while the generator is in the underexcited region. When the AVR manual mode status indication is available, Zone 3 will issue an accelerated trip as described in Section VI.

B. Case Study 2: Generator Trip During UEL Testing

Reference [14] also describes an event of an LOF misoperation during testing of the UEL at 90 percent of rated generator MVA. Because the generator operating point encroached into the Zone 2 characteristic of the impedance LOF element, as shown in Fig. 25, the generator tripped. In this AVR, the UEL characteristic is fixed in the P-Q plane. When $V_T = 0.95$ pu, the LOF element Zone 2 characteristic encroached into the UEL characteristic and timed out.
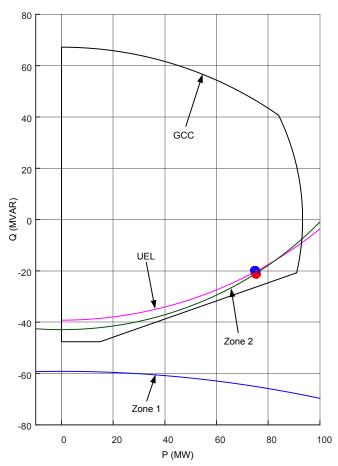

Fig. 25. The operating point entered Zone 2 ($V_T = 0.95$ pu) during UEL testing, causing an undesired generator trip.

Typically, CFE sets the UEL characteristic between 90 and 95 percent of the GCC in the underexcited region. SECHL is the main constraint in the underexcited region for this type of generator, so CFE sets the Zone 2 impedance LOF element based on the GCC. To avoid incorrect operation of the LOF element under these conditions, CFE recalculated the Zone 2 reach by increasing the GCC values to 110 percent of the original GCC in the underexcited region.

As the previous section described, when we use the P-Q plane for LOF protection, we can set the Zone 2 characteristic identically to the UEL. For this event, the Zone 2 setting margin would have placed the generator operating point outside of the Zone 2 characteristic. The advantage of the P-Q plane approach is that the Zone 2 element can be set to respond identically to the UEL with respect to V_T (if we use $k = 0$ for this application). In this manner, we can maintain grading between the UEL and the Zone 2 element. On the other hand, in the case of the impedance element we know that impedance is directly proportional to V_T^2, so we can achieve coordination at the expense of the GCC margin.

C. Case Study 3: LOF Condition by the Opening of the Field Winding

This event demonstrates the operation of the proposed LOF elements when the field winding of a salient-pole generator is open-circuited, as shown in Fig. 26. Table I shows the machine parameters.

Fig. 26. LOF condition resulting from open-circuited field winding.

TABLE I
PARAMETERS OF THE GENERATOR

MVA Rating	23.5 MVA
Nominal Current	2056 A
Nominal Voltage	6.6 kV
X_d	0.9 pu
X'_d	0.315 pu

Fig. 27 shows V_T, I_T, P, and Q for the generator before and during the open-circuited field condition. With the field winding open, V_T drops rapidly below 0.7 pu, as shown in Fig. 27. The momentary drop in power because of this condition causes the generator rotor to accelerate with a significant slip. This slip induces currents in the damper windings. In this case, the generator impedance changes from X_d to a value approximately equal to X'_d. Therefore, the SSSL, which is based on X_d, does not properly represent the actual stability limit. Hence, the generator did not lose stability and did not slip poles even after crossing the Zone 2 characteristic.

We analyzed this event in the admittance plane because Zone 1 and Zone 3 operate in the admittance plane, as shown in Fig. 28. Zone 2 can operate in either the P-Q plane ($k = 0$) or the admittance plane ($k = 2$) to coordinate with the UEL characteristic. Zone 1 would have operated for this severe LOF to prevent pole slipping, as shown in Fig. 27 and Fig. 28.
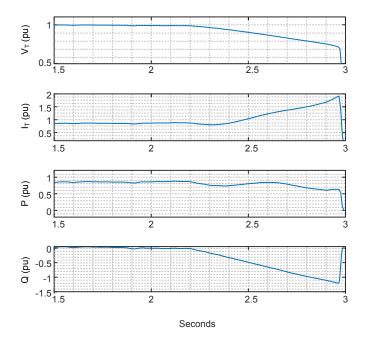
Fig. 27. Response of the generator during an open-circuited field condition; V_T, I_T, P, and Q.
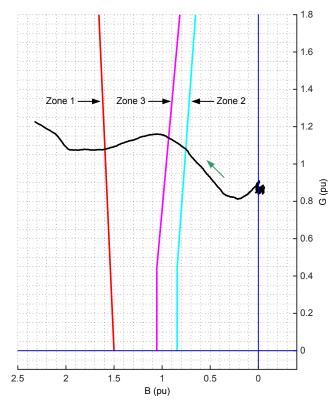

Fig. 28. Operating point trajectory in the admittance plane for a complete generator LOF condition.

VIII. Conclusions

The first generation of LOF protection schemes was developed decades ago. At that time, excitation systems and AVRs were simpler and system stability was the major concern. Legacy LOF protection schemes provided good operating speed for most LOF events and were secure for external faults and power swings. They used electromechanical technology, so implementation was also simple. However, these legacy schemes left room for improvement.

This paper introduces a new LOF protection scheme that provides better protection without sacrificing the advantages of legacy implementations. The proposed scheme is built around the concept of a GCC replica. Generator capability changes with cooling conditions. Modern generators have instrumentation that provides analog indication of the cooling condition. The scheme can use these analog measurements to dynamically expand and contract the GCC replica.

SECHL is a problem for cylindrical-rotor machines and it varies with V_T. Modern UELs can shift their characteristics to match the GCC. The Zone 2 and Zone 4 elements this paper introduces have characteristics that can shift in the same direction and degree as the UEL characteristic. This adaptation allows for a smaller margin between the UEL and LOF element characteristics, resulting in better protection for the generator.

LOF schemes also provide protection against loss of steady-state stability, and for this reason legacy schemes are often coordinated with the SSSL characteristic in addition to the UEL characteristic, which may compromise the generator LOF protection. The new LOF scheme includes a dedicated zone (Zone 3) to coordinate with the SSSL characteristic for improved coordination without sacrificing generator protection.

Finally, the new LOF scheme is defined in the P-Q plane, which eases setting of elements. You can enter the required scheme settings with the values obtained from the generator data sheet. Additionally, a graphical user interface that displays the relay characteristics and provides assurance that the scheme is properly configured. This approach reduces the possibility of setting errors.

IX.   APPENDIX

A.   Example 1

Table II shows the LOF scheme settings for the application with voltage-independent UEL (k = 0) described in Section VI, Subsection E.

TABLE II
UEL WITH k = 0

Zone 1 Per Impedance Scheme 2		Coordination of UEL and Zone 2 Characteristics				SSSL Characteristic	
Zone 1 Settings	Value	UEL Settings in AVR [P, Q] (Primary)	Zone 2 Settings	Value (Primary)		Zone 3 Settings	Value (pu)
40P1P	0.6 pu	[40, −12.6]	[UELP1, UELQ1]	[40, −12.6]		X_d	1.8
Tilt	−5 deg	[20, −18]	[UELP2, UELQ2]	[20, −18]		X_S	0.2
		[0, −19.8]	[UELP3, UELQ3]	[0, −19.8]		Voltage Acceleration	0.8
			Margin	10%			
			Characteristic	Linear			
			Voltage dependency (k)	0			

B.   Example 2

Table III shows the LOF scheme settings for the application with voltage-dependent UEL (k = 1) described in Section VI, Subsection E.

TABLE III
UEL WITH k = 1

Zone 1 Per Impedance Scheme 1		Coordination of UEL and Zone 2 Characteristics				SSSL Characteristic	
Zone 1 Settings	Value	UEL Settings in AVR [P, Q] (Primary)	Zone 2 Settings	Value (Primary)		Zone 3 Settings	Value (pu)
40P1P	0.95 pu	[40, −12.6]	[UELP1, UELQ1]	[40, −12.6]		X_d	1.8
Tilt	−5 deg	[20, −18]	[UELP2, UELQ2]	[20, −18]		X_S	0.2
		[0, −19.8]	[UELP3, UELQ3]	[0, −19.8]		Voltage Acceleration	0.8
			Margin	10%			
			Characteristic	Quadratic			
			Voltage Dependency (k)	1			

X. ACKNOWLEDGMENT

The authors appreciate the help of Paulo Lima from SEL and M. Sosa-Aguiluz from CFE for providing the events for our analysis.

XI. REFERENCES

[1] S. B. Farnham and R. W. Swarthout, "Field Excitation in Relation to Machine and System Operation," *Transactions of the American Institute of Electrical Engineers*, Vol 72, Part III, Issue 6, December 1953, pp. 1215–1223.

[2] IEEE Standard C50.12–2005 (Previously designated as ANSI C50.12-1982), Standard for Salient-Pole 50 Hz and 60 Hz Synchronous Generators and Generator/Motors for Hydraulic Turbine Applications Rated 5 MVA and Above.

[3] IEEE Standard C50.13-2014 (Revision of IEEE Standard C50.13-2005), IEEE Standard for Cylindrical-Rotor 50 Hz and 60 Hz Synchronous Generators Rated 10 MVA and Above.

[4] Generator Control Testing to Certify Reactive Power Capability, Excitation System Functions and Frequency Response, Guidelines for NERC Compliance, Product Id: 1014911, November 29, 2007.

[5] S. S. Choy and X. M. Xia, "Under Excitation Limiter and Its Role in Preventing Excessive Synchronous Generator Stator End-Core Heating," *IEEE Transactions on Power Systems*, Vol. 15, Issue 1, February 2000, pp. 95–101.

[6] D. Reimert, *Protective Relaying for Power Generation Systems*. CRC Press Taylor & Francis Group, Boca Raton, Florida, 2006.

[7] G. Benmouyal, "The Impact of Synchronous Generators Excitation Supply on Protection and Relays," proceedings of the 34th Annual Western Protective Relay Conference, Spokane, WA, October 2007.

[8] F. P. DeMello and C. Concordia, "Concepts of Synchronous Machine Stability as Affected by Excitation Control," *IEEE Transactions on Power Apparatus and Systems*, Vol. PAS–88, Issue 4, April 1969, pp. 316–329.

[9] R. Sandoval, A. Guzmán, and H. J. Altuve, "Dynamic Simulations Help Improve Generator Protection," proceedings of the 33rd Annual Western Protective Relay Conference, Spokane, WA, October 2006.

[10] G. R. Berube and L. M. Hajagos, "Coordination of Under Excitation Limiters and Loss of Excitation Relays With Generator Capability," 2009 IEEE Power & Energy Society General Meeting, Calgary, AB, 2009, pp.1–8.

[11] C. R. Mason, "A New Loss-of-Excitation Relay for Synchronous Generators," *Transactions of the American Institute of Electrical Engineers*, Vol. 68, Issue 2, July 1949, pp. 1240–1245.

[12] J. Berdy, "Loss-of-Excitation Protection for Modern Synchronous Generators," *IEEE Transactions on Power Apparatus and Systems*, Vol. PAS–94, Issue 5, September 1975, pp. 1457–1463.

[13] IEEE Standard C37.102-2006, IEEE Guide for AC Generator Protection.

[14] M. Sosa-Aguiluz, A. Guzmán, and J. León, "CFE Generator Protection Guidelines for Setting 40 and 64G Elements Based on Simulations and Field Experience," proceedings of the 41st Annual Western Protective Relay Conference, Spokane, WA, October 2014.

[15] R. L. Tremaine and J. L. Blackburn, "Loss-of-Field Protection for Synchronous Machines [includes discussion]," *Transactions of the American Institute of Electrical Engineers. Part III: Power Apparatus and Systems*, Vol. 73, Issue 1, Jan. 1954, pp. 765–777.

[16] H.-J. Hermann and D. Gao, "Underexcitation Protection Based on Admittance Measurement – Excellent Adaptation on Capability Curves," 1st International Conference on Hydropower Technology and Key Equipment, Beijing, China, 2006. Available: http://www.lici.com.cn/asp/ext/images/78.pdf?iydlfad=38966.

[17] J. H. Walker, "Operating Characteristics of Salient-Pole Machines," *Proceedings of the IEE – Part II*, Vol. 100, Issue 73, 1953, p. 13.

[18] IEEE Standard 421.5-2016 (Revision of IEEE Standard 421.5-2005), IEEE Recommended Practice for Excitation System Models for Power System Stability Studies.

[19] NERC Reliability Standard PRC-026–1, Relay Performance During Stable Power Swings.

XII. BIOGRAPHIES

Matchyaraju Alla received his bachelor of engineering degree from Gitam University, India, in 2010 and his master of engineering degree from the University of Idaho, USA, in 2017. He received his post-graduate diploma in thermal power plant engineering from National Power Training Institute, India, in 2012. He began his career with Vedanta Resources Plc, where he worked in generator protection and control and was in charge of testing and commissioning three 660 MW thermal power plants. Since 2016, Mr. Raju has been employed as a power engineer with Schweitzer Engineering Laboratories Inc. His areas of interest include generator protection, transformer protection, and motor protection. He is a member of IEEE.

Armando Guzmán received his BSEE with honors from Guadalajara Autonomous University (UAG), Mexico. He received a diploma in fiber-optics engineering from Monterrey Institute of Technology and Advanced Studies (ITESM), Mexico, and his masters of science and PhD in electrical engineering and masters in computer engineering from the University of Idaho, USA. He served as regional supervisor of the Protection Department in the Western Transmission Region of the Federal Electricity Commission (the electrical utility company of Mexico) in Guadalajara, Mexico for 13 years. He lectured at UAG and the University of Idaho in power system protection and power system stability. Since 1993 he has been with Schweitzer Engineering Laboratories, Inc. in Pullman, Washington, where he is a fellow research engineer. He holds numerous patents in power system protection and synchrophasor and fault locating technology. He is a senior member of IEEE.

Dale Finney received his bachelor of engineering degree from Lakehead University and his master of engineering degree from the University of Toronto. He began his career with Ontario Hydro, where he worked as a protection and control engineer. Currently, Mr. Finney is employed as a principal power engineer with Schweitzer Engineering Laboratories, Inc. His areas of interest include generator protection, line protection, and substation automation. Mr. Finney holds more than ten patents and has authored more than 30 papers in the area of power system protection. He is a member of the main committee and vice-chair of the rotating machinery subcommittee of the IEEE PSRC. He is a senior member of the IEEE and a registered professional engineer in the province of Nova Scotia.

Normann Fischer received a Higher Diploma in Technology, with honors, from Technikon Witwatersrand, Johannesburg, South Africa, in 1988; a BSEE, with honors, from the University of Cape Town in 1993; an MSEE from the University of Idaho in 2005; and a PhD from the University of Idaho in 2014. He joined Eskom as a protection technician in 1984 and was a senior design engineer in the Eskom protection design department for three years. He then joined IST Energy as a senior design engineer in 1996. In 1999, Normann joined Schweitzer Engineering Laboratories, Inc., where he is currently a fellow engineer in the research and development division. He was a registered professional engineer in South Africa and a member of the South African Institute of Electrical Engineers. He is currently a senior member of IEEE and a member of the American Society for Engineering Education (ASEE). Normann has authored over 60 technical and 10 transaction papers and 22 patents (2 pending) related to electrical engineering and power system protection.